Research Article

Hua Yu#, Liangliang Zhang*#, Fangfang Cai, Sujuan Zhong, Jia Ma, Li Bao, Yongtao Jiu, Bingli Hu, Shizhong Wei*, and Weimin Long*

Microstructure and mechanical properties of brazing joint of silver-based composite filler metal

https://doi.org/10.1515/ntrev-2020-0083
received September 7, 2020; accepted September 29, 2020

Abstract: In this article, environmental friendly BAg25 Cu40Zn34Sn (BAg-25) and BAg30Cu37Zn32Sn (BAg-30) flux-core solder metal capable of facilitating automatic production of brazing manufacturing processes were prepared. The butt and lap induction brazing tests were carried out on the substrate with BAg-25 and BAg-30. Wettability, microstructure and mechanical properties of the solders on the base metal were studied by field emission scanning electron microscope (SEM-EDS), electron backscattering diffraction (EBSD), tensile testing machine and microhardness tester. Results indicated that the wetting property of BAg-30 with 30% silver content was better than that of BAg-25 with 25% silver content. At the same time, besides copper and silver-based solid solutions, the brazed joint of BAg-30 solder also contain Cu + Ag eutectic phase. In the brazed joint of BAg-25 solder, the grain size is smaller, which makes the tensile strength and the shear strength of the joints better. Therefore, the BAg-25 flux-core solder metal will further reduce the industrial cost and meet the requirements of mechanical properties.

Keywords: composite filler metal, induction brazing, wettability, microstructure, grain refinement

# These authors contributed equally to this work and should be considered first co-authors.

*** Corresponding author: Liangliang Zhang,** School of Material Science & Engineering, Henan University of Science and Technology, Luoyang, 471000, China; National Joint Engineering Research Center for Abrasion Control and Molding of Metal Materials, Luoyang, 471000, China, e-mail: zll15538029120@163.com
*** Corresponding author: Shizhong Wei,** School of Material Science & Engineering, Henan University of Science and Technology, Luoyang, 471000, China; National Joint Engineering Research Center for Abrasion Control and Molding of Metal Materials, Luoyang, 471000, China, e-mail: wsz@haust.edu.cn
*** Corresponding author: Weimin Long,** Zhengzhou Research Institute of Mechanical Engineering Co. Ltd, Zhengzhou, 450000, China, e-mail: brazelong@163.com
Hua Yu, Fangfang Cai: School of Material Science & Engineering, Henan University of Science and Technology, Luoyang, 471000, China; National Joint Engineering Research Center for Abrasion Control and Molding of Metal Materials, Luoyang, 471000, China
Sujuan Zhong: National Joint Engineering Research Center for Abrasion Control and Molding of Metal Materials, Luoyang, 471000, China; Zhengzhou Research Institute of Mechanical Engineering Co. Ltd, Zhengzhou, 450000, China
Jia Ma, Li Bao, Yongtao Jiu: Zhengzhou Research Institute of Mechanical Engineering Co. Ltd, Zhengzhou, 450000, China
Bingli Hu: School of Material Science & Engineering, Henan University of Science and Technology, Luoyang, 471000, China

1 Introduction

Ag–Cu–Zn brazing filler metal is widely used to weld various steels, high temperature nickel-based alloys, copper-based alloys, and other materials [1] due to its good electrical conductivity [2], thermal conductivity [3], low melting point [4], high strength and corrosion resistance [5]. The addition of Cu element in the silver base solder can reduce the melting temperature of Ag base solder [6], and at the same time, a variety of elements can be fixed to form a solid solution rather than brittle phases [7]. The addition of Zn and other metal elements in the silver base filler metal is beneficial to form a ternary alloy [8], which can further reduce the liquidus temperature of the filler metal and improve the brazing performance of the filler metal [9]. However, as a precious metal for silver, lots of additions in Ag–Cu–Zn solder limit its widespread applications on braze welding. Therefore, Yijie et al. [10] prepared the Ag–Cu–Zn–Cd solder by adding the element Cd to lower the Ag content. It was concluded that adding Cd effectively reduced the liquidus temperature of the solder and helped to only

form Ag-based and Cu-based solid solutions instead of hard brittle phases, obtaining the enhanced plastic processing performance of the solder [11]. However, Cd was listed as the seventh hazardous substance to human health by the World Health Organization. Hence, Schnee et al. [12] synthesized Ag–Cu–Zn–Sn filler metal by using Sn instead of Cd and found that Sn could reduce the solidity and liquidus of the filler metal and improve the wettability of the filler metal. Daniel S of Umicore also prepared BAg43-CuZnMnSn solder [13]. However, with the increase of the Sn content, there is a certain proportion of brittle phase in the microstructure of brazing filler metal, which seriously affects the mechanical properties of brazed joint [14]. Therefore, controlling the content of Sn in solder is a hot spot in the field of brazing research [15].

However, during the brazing process, the composite application form of brazing filler metal and brazing flux is usually the use of solid brazing flux immersion. This method increases the prewelding procedure and operation time, and the controllability gets worse, which affects the consistency and the quality stability of the welding [16]. Moreover, to ensure the quality of brazing, excessive brazing agent has to be added, which cause other nonnegligible problems such as polluting the air, endangering the health of operators and excessive consumption of brazing agent [17]. Therefore, the new silver-based composite filler metal Ag–Cu–Zn–Sn recommended in this study meets the requirements of green manufacturing and is suitable for automatic and intelligent welding technology [18]. Related research shows that compared with traditional filler metals, flux filler metals can improve production efficiency and brazing quality [19].

In this article, the wettability, microstructure and phase evolution were studied, and the enhancement performance and the corresponding mechanism were analyzed.

2 Experimental procedures

The matrix material Q235A used for the wettability test was 40 × 40 × 3 (mm), and the matrix material used for induction brazing test was 70 × 20 × 3 (mm). The components of BAg-25 and BAg-30, the new type of solders used in the test, are presented in Table 1. Before induction brazing, the wettability of the solder on the base metal was measured to obtain the best wettability. The heating treatment was conducted for 30 s in a box-type resistance furnace (SX2-10-12G) with a heating temperature rating of 1,200, a power of 10 kW and a voltage of 380 v. According to the standard GB/t 11364-2008, the wettability of solder was tested. The dosage of solder and brazing agent are 0.2 and 0.15 g, respectively. Before brazing, the surface of the substrate is polished with sandpaper to remove oily impurities and oxides, which are considered to affect the wettability of substrate [20] and then cleaned in the acetone solution by ultrasonic. At the same time, mark a scale on the filler metal at intervals of 20 mm to quantify the filler metal in the welding process.

Table 1: Chemical composition of silver-based composite filler metals

Materials	Ag	Cu	Zn	Sn
BAg25TS	25	40	34	1
BAg30T	30	37	32	1

For induction brazing, butt joint and lap joint are adopted. The lap length of the joint is 5 mm, and the base material was fixed on the special fixture according to the lap length and butt joint. After the joint is heated to the optimum wetting temperature and kept for 10 s, the brazing is carried out in an induction brazing machine. After the joints are cooled to room temperature in air, the residual brazing flux on the joint surface is removed by mechanical cleaning [21].

The tensile strength and the shear strength of joints were tested on a precision universal electronic tensile testing machine (AG-I250KN SHIMADZU). Scanning electron microscope (SEM, JSM-560LV) and energy dispersive spectrometer were used to study the interface morphology and phase evolution of the brazed joint. The hardness of the cross section of brazed joints was measured on a microhardness tester.

3 Results and discussion

3.1 Wettability of silver based composite solder

Wetting and spreading experiments were carried out on the base metals of BAg-25 and BAg-30 for 30 s at 800, 825, 850 and 875, respectively. Figure 1(a) shows that the wettability of BAg-30 on the base metal is better, and the overall spreading area is larger than that of BAg-25. The wetting areas of the two kinds of solder alloys reached the maximum at 850°C, being 374 and 275 mm^2,

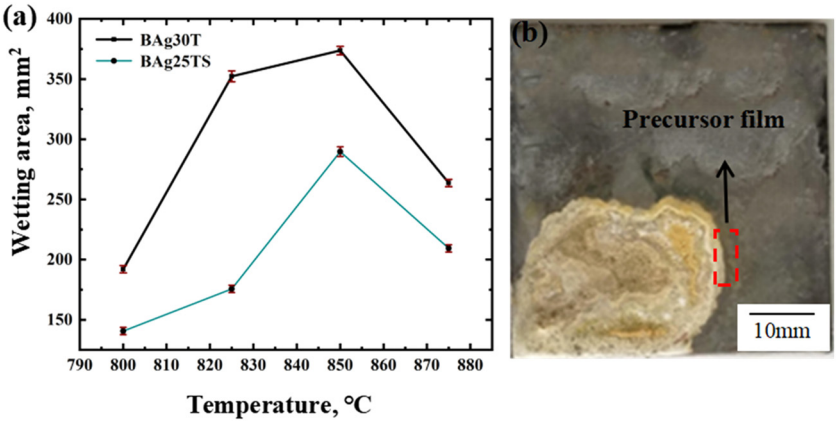

Figure 1: (a) Wetting area curve and (b) wetting and spreading image of brazing joints.

respectively. When the temperature is lower than 850°C, the wetting areas of the two kinds of filler metals increase with the increase of temperature, and when the temperature exceeds 850°C, the wetting areas decrease sharply. It can be seen from the image of wetting and spreading of BAg-30 solders on the base metal in Figure 1(b), BAg-30 was proved to have good wettability, which was proved by a bright white precursor film outside the metal filling. The filler metal with wider precursor film has lower viscosity and better fluidity. Preferential spreading of the precursor film reduces the surface tension between the solder and the base metal, which makes the spread area of the filler metal for BAg-30 welding larger [22]. When the temperature continues to increase, the temperature in the furnace is higher than the flux protection temperature, which leads to flux failure and serious oxidation of basic filler metal, resulting in poor wettability of the flux filler material [23].

3.2 Microstructure of brazing joint of silver-based composite filler metal

The SEM images of BAg-25 and BAg-30 brazing joints of silver-based composite filler metals are shown in Figure 2. The left substrate Q235 and the right brazing joint are welded and fused together, forming a good intersecting surface without microcracks and slag inclusion. In Figure 2(a), gray-black clusters with the size of 6–12 μm are irregularly surrounded by small-sized gray-black phases. In Figure 2(b), except for the presence of larger-sized gray-black and gray-white phases, the needle substance was found to be interwoven with gray-white phase. In the range of 8–20 μm, the size of gray-black clusters is larger than that shown in Figure 2(a). The chemical compositions of the three phases by the energy spectrum analysis are listed in Table 2. The lumpy gray-black phase shown in Figure 2(a) and (b) is the Cu-based solid solution [24], while the gray-white phase and needle-like substance are analyzed as Ag-based solid solution and (Cu + Ag) eutectic phase, respectively, which is consistent with Ref. [25].

The scanning results of the energy spectrum of the brazed joint are shown in Figure 2(c–f). According to the phase diagrams of Cu–Fe and Fe–Zn at 850°C, both Cu and Zn can dissolve in the base metal Fe, where the solid solubility of Zn is higher than that of Cu [26]. However, Ag in the solder cannot dissolve in α-Fe [27]. The comparison of the line scanning results in Figure 2(e) and (f) shows that the degree of diffusion of Cu, Ag and Zn in the brazed joint of BAg-30 is higher than that of Cu, Ag and Zn in the brazed joint of BAg-25. At the same time, the scan results of the energy spectrum show that the step-like scanning area where copper element can be higher than silver element is copper-based solid solution [28]. However, in the results of energy spectrum scanning, the concave–convex scanning area where the silver element is higher than the copper element is the silver-based solid solution. In Figure 2(f), which is a typical Ag–Cu eutectic region [29], is not only the linear scanning region corresponding to Cu-based solid solution and Ag-based solid solution but also the region corresponding to the peak value of Ag and the lowest value of Cu energy spectrum scanning curve [30].

To clearly illustrate the formation modes of Cu-based solid solution and Ag-based solid solution in the brazing process, Figure 3 shows the crystal cell model of the two solid solution forming processes. In the periodic table, Cu and Zn are in the same element period, while Ag and Zn are in different element periods. The difference in atomic

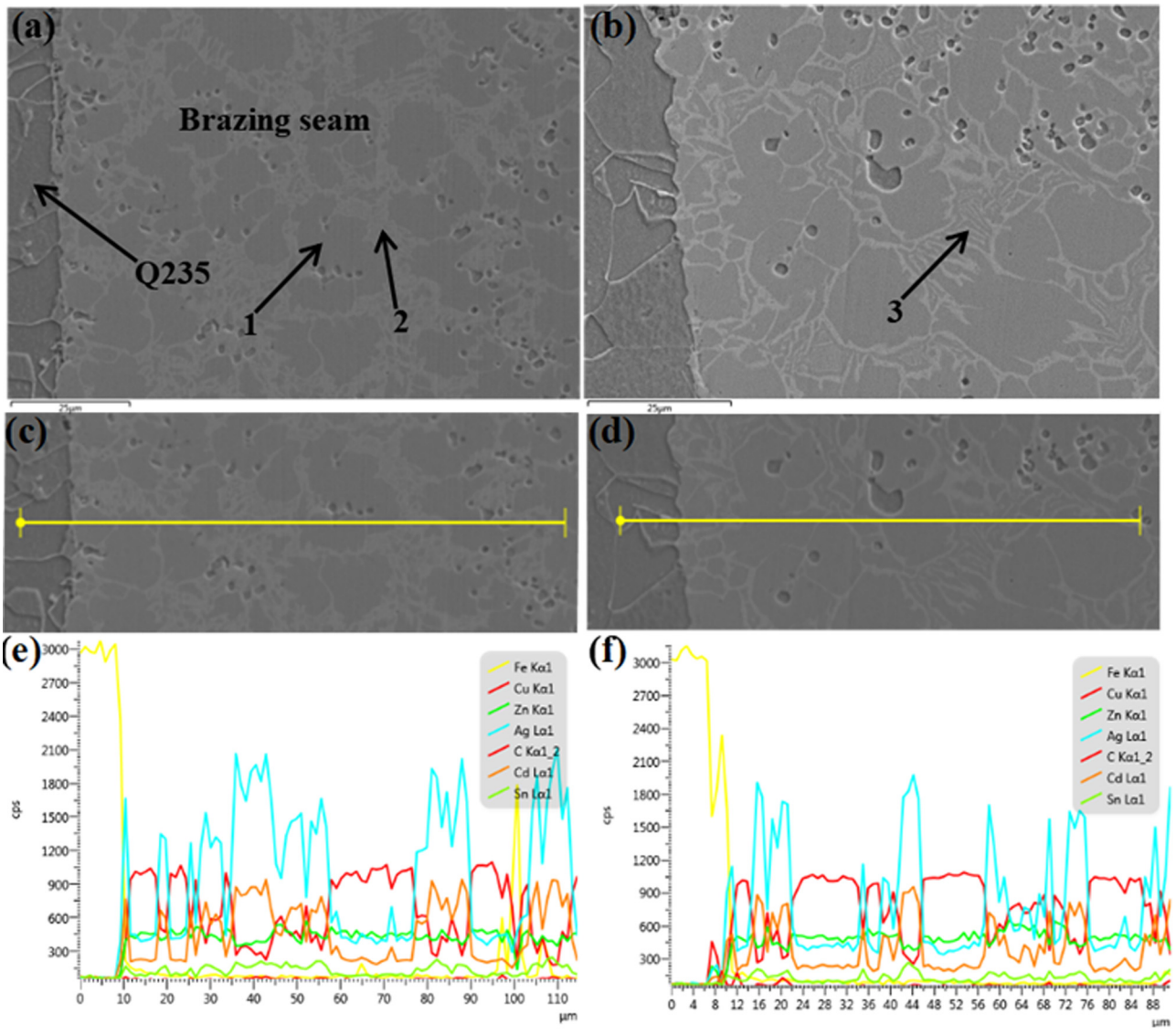

Figure 2: SEM images of (a) BAg25TS brazing joint; (b) BAg30T brazing joint; (c and d) BAg25TS, BAg30T brazing joint line scanning position and (e and f) line scan results.

Table 2: Mass phase energy spectrum of brazing joint of silver-based composite core filler metal

Point	W(Ag)	W(Cu)	W(Zn)	W(Sn)	W(other)
1	15.1	57.2	27.7	—	—
2	71.8	5.9	22.3	—	—
3	57.8	19.5	19.7	2.5	0.5

diameter percentage between Cu and Zn is smaller than that of Ag and Zn, and the solid solubility of Zn in Cu is greater than that of Zn in Ag [31]. Therefore, as the temperature decreases, the solid solution composed of Cu and Zn with high melting point crystallizes first [32]. With the solidification process going on, the content of residual Cu and Zn atoms in the liquid phase decreases. Finally, Cu and Zn are dissolved in Ag with low melting point, forming silver-based solid solution. When the temperature drops to the eutectic point, the remaining liquid phase forms (Cu + Ag) the eutectic structure [33]. Figure 4 shows the EBSD micrographs of the solder joint, and Figure 4(a) and (b) shows the texture direction of the joint. Figure 5 is the pole diagram of each phase in the brazed joint. Different colors can show different texture directions. Figure 4(c) and (d) are the inverse pole figure of each phase in Figure 4(a) and (b). It can be seen from the figure that the two kinds of brazing filler metals do not form texture with specific orientation during brazing

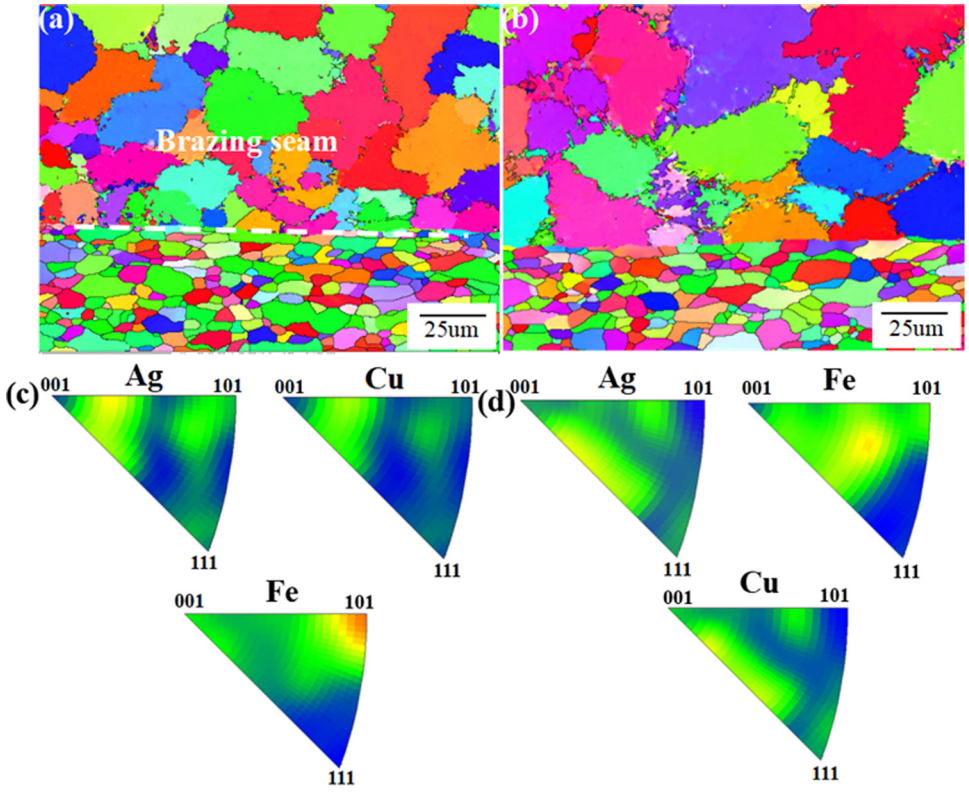

Figure 3: EBSD images of samples of (a) BAg25TS; (b) BAg30T and (c and d) inverse pole figure.

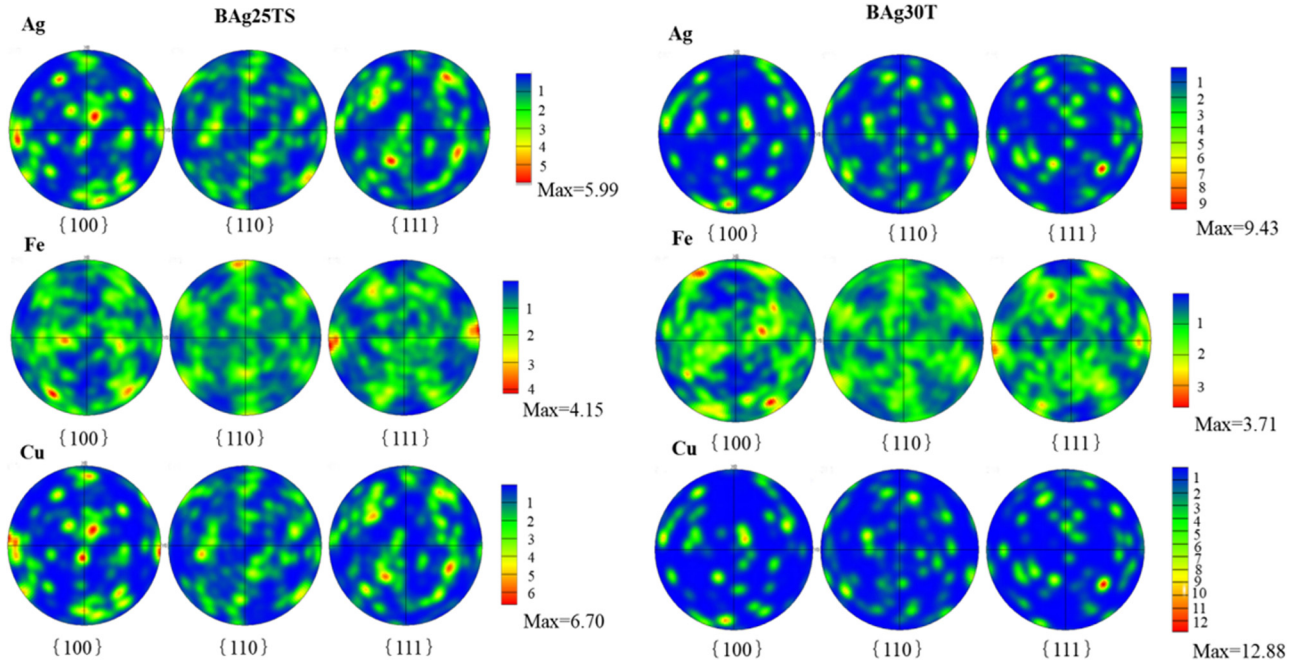

Figure 4: Pole figures of Cu-based solid solution (Cu), Ag-based solid solution (Ag), α-Fe phase (Fe) in BAg25TS and BAg30T brazing joints.

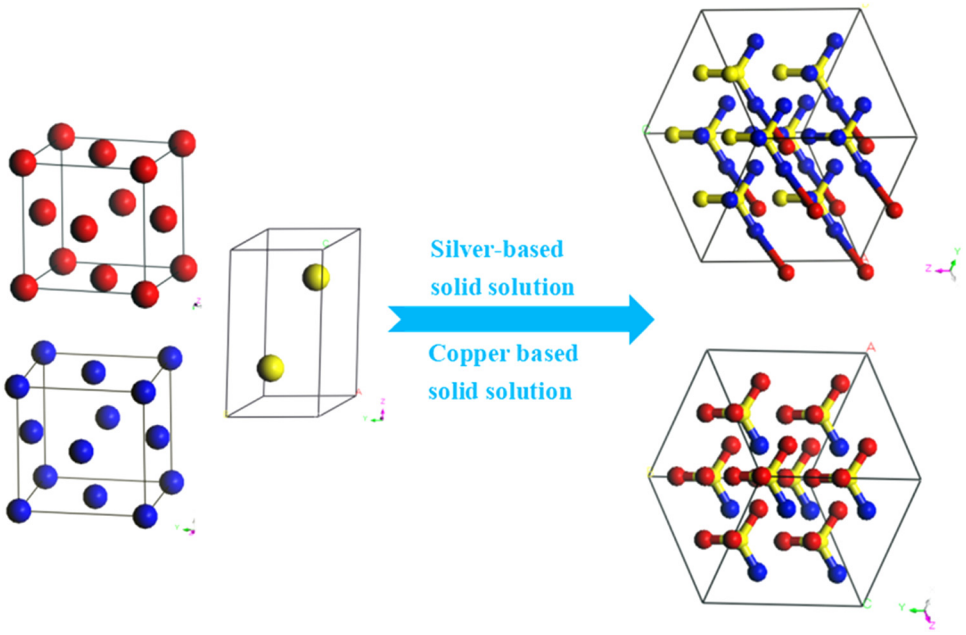

Figure 5: Cell model diagram of the formation process of copper and silver-based solid solutions.

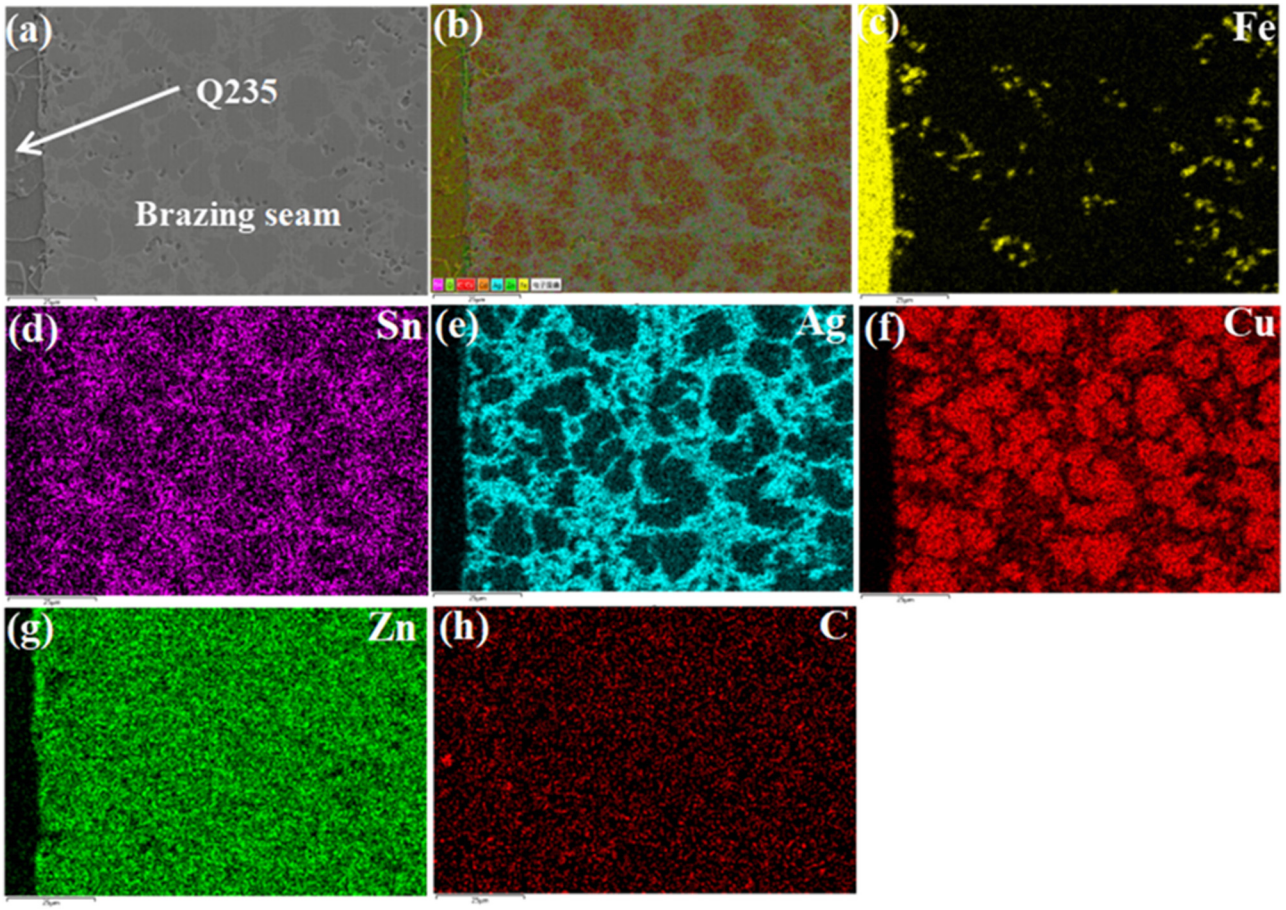

Figure 6: EDS distribution diagram of brazing joints interface at BAg25TS brazing joint. (a) cross section morphology of brazed joints; (b) surface scanning; (c) Fe; (d) Sn; (e) Ag; (f) Cu; (g) Zn; (H) C.

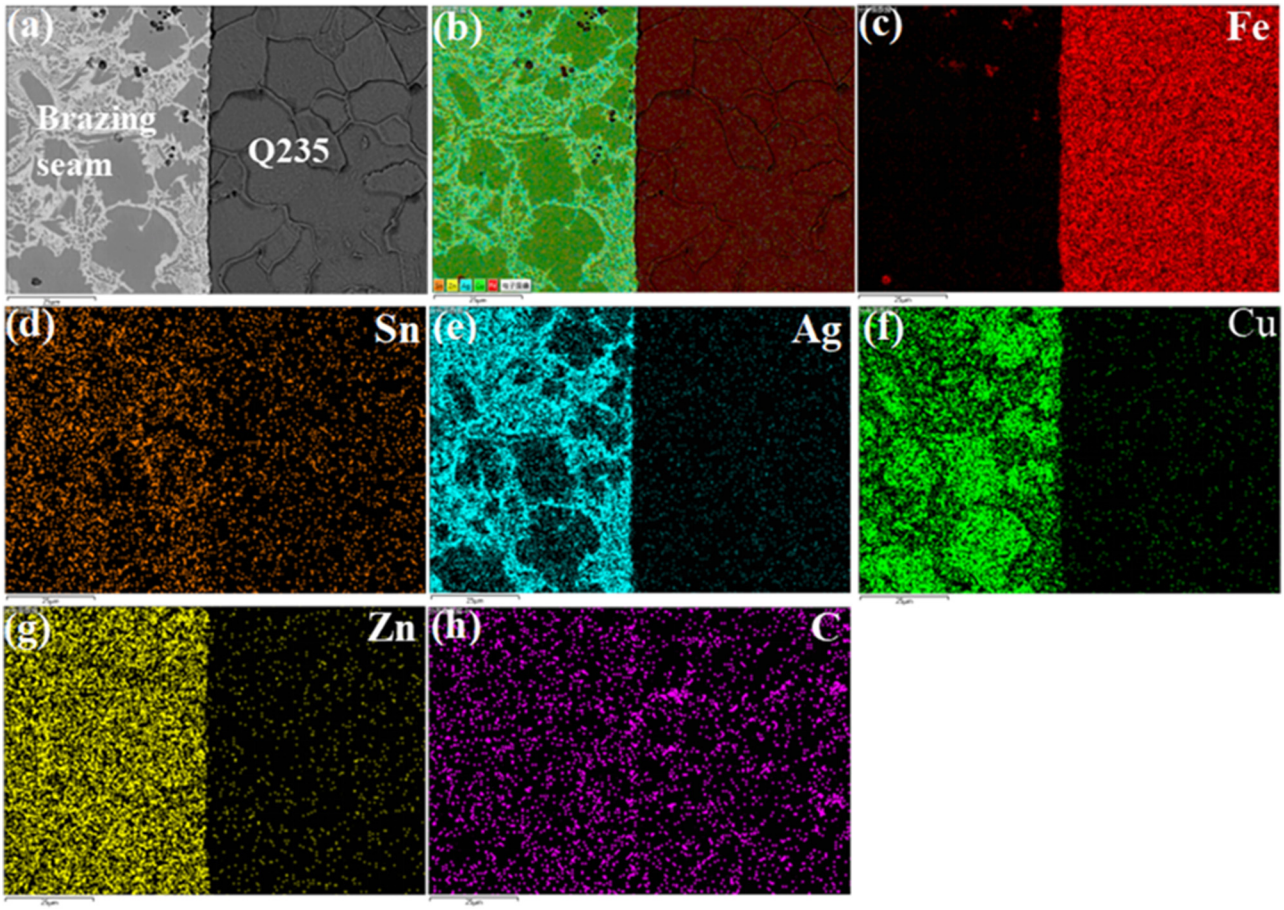

Figure 7: EDS distribution diagram of brazing joints interface at BAg30T brazing joint. (a) Cross section morphology of brazed joints; (b) surface scanning; (c) Fe; (d) Sn; (e) Ag; (f) Cu; (g) Zn; (H) C.

[34], and the grain size in the brazing joint of BAg-30 is significantly larger than that in the brazing joint of BAg-25 [35].

The scanning results of the energy spectrum of the brazing joint of the silver base filler metal are shown in Figures 6 and 7. By comparing the distribution of the Sn element in Figures 6(d) and 7(d) at the interface of the brazing joint, it can be found that the Sn element is evenly distributed at the interface of the brazing joint. By observing distribution of copper and silver elements in brazed joints and comparing Figure 6(e) and (f) with Figure 7(e) and (f), it can be found that the interface Cu element in the brazing joint using BAg-25 brazing filler metal is distributed in a cluster, while Ag element is closely distributed around the cluster Cu element and connected to each other. However, in the brazed joint using BAg-30 brazing filler metal, the clubbed Cu element is not as uniformly distributed as shown in Figure 6(f), which is consistent with the phenomenon that the size of Cu-based solid solution is smaller in the brazing joint using BAg-25 filler metal shown in Figure 2(a). By comparing Figures 6(g) and 7(g), it can be found

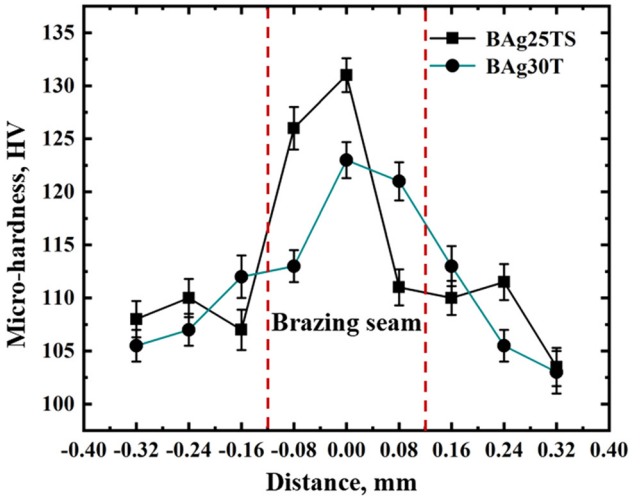

Figure 8: Microhardness of brazing joint of silver base composite filler metal.

that the Zn element is uniformly distributed in the Cu-based solid solution, Ag-based solid solution and (Cu + Ag) eutectic phase without segregation [36].

3.3 Mechanical properties of brazing joint with silver-based composite filler metal

The microhardness of the brazed joint was measured by a HV-1000 microhardness tester. The test load was 200 gf, and the loading time was 10 s. The microhardness curve of brazed joints and interface are shown in Figure 8. Figure 8 shows that the hardness values of the brazing joints in the two brazing joints are significantly higher than that of the base metal. The mean microhardness of the highest point of BAg-25 is 132.8 HV, while that at BAg-30 is 125.8 HV. The microhardness of BAg-25 is higher than that of BAg-30.

AG-I250KN SHIMADZU precision universal electronic tensile testing machine was used to test the tensile strength and the shear strength of the brazed joint. The results of the tensile test are shown in Figure 9(a), and the shear strength and the tensile strength are shown in Figure 9(b). During the process of the shear test, the specimen with the overlapping length of 5 mm finally broke at the overlapping surface. Figure 9(a) and (b) show that the average tensile strength of the brazing joint of BAg-25 is 206 MPa, which is higher than the average 172 MPa of the brazing joint of BAg-25, and the shear strength of BAg-25 is 116 MPa, which is significantly higher than the shear strength of BAg-30 brazing joint. However, the experimental results are discrete. To quantitatively analyze its mechanical properties, a two-parameter Weibull distribution model is introduced [37]:

$$P(X) = 1 - \exp\left[-\left(\frac{x}{\beta}\right)^{\alpha}\right] \tag{1}$$

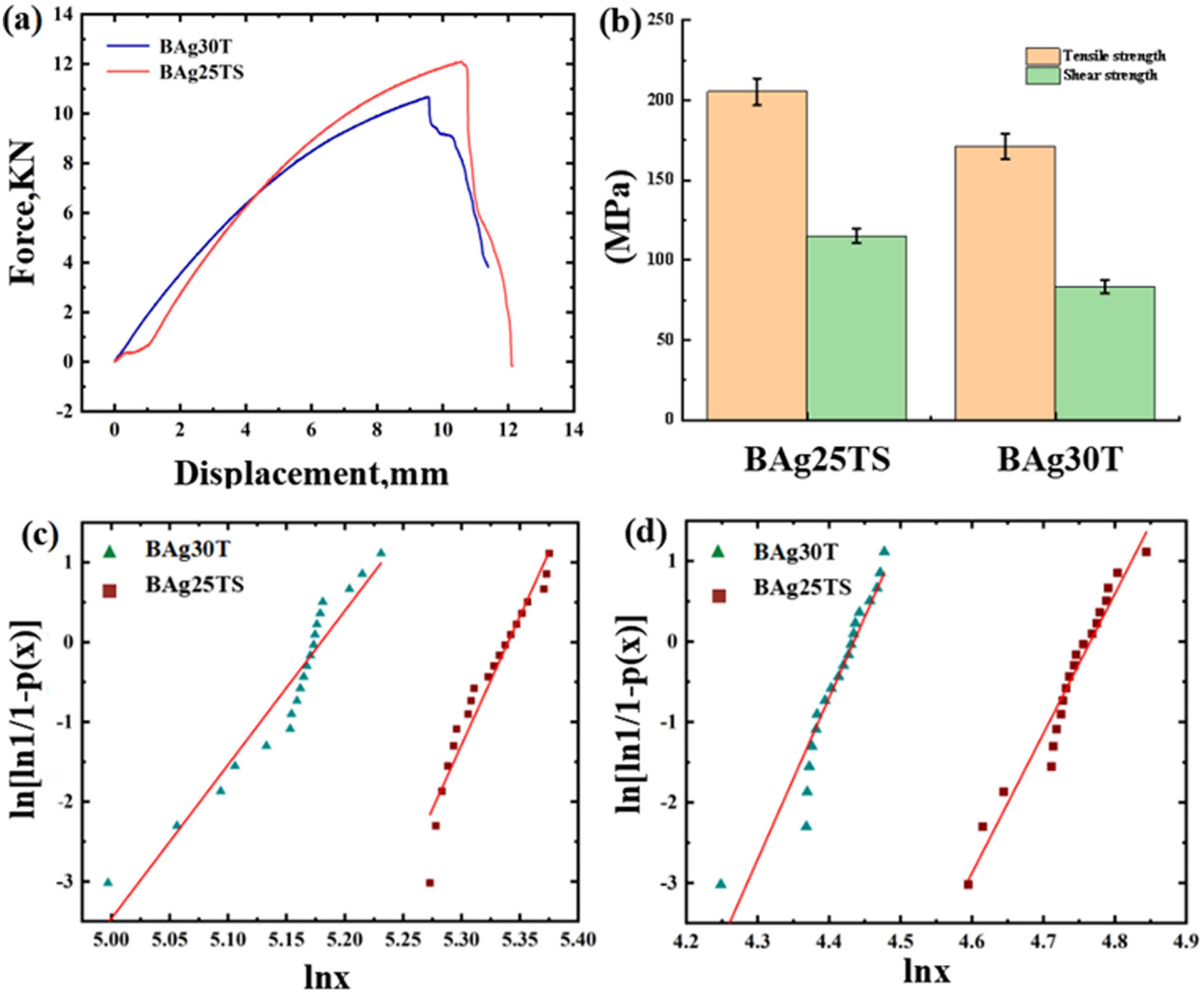

Figure 9: (a) Force–displacement curve of brazing joint and (b) columnar diagram of tensile strength and shear strength of brazing joint. Weibull distribution of (c) tensile strength and (d) shear strength of brazed joint.

where β are the ruler parameter, indicating the characteristic strength of the material; α is the Weibull modulus, reflecting the intensity dispersion. The statistical sample size for each experiment was about 20. In the ascending order of tensile strength and shear strength, the corresponding probability of fracture is $P_i = \frac{i}{n+1}$, where i is the ordinal number of the ascending order and n is the total number of samples. When the Weibull function is fitted to the sample, equation (1) can be transformed into

$$\ln[\ln(1-p)^{-1}] = \alpha \ln x - \alpha \ln \beta. \quad (2)$$

According to the experimental data, the Weibull distribution parameters β and α are obtained by using the least square method [38]. The results of the tensile test and the shear test of brazed joints using BAg-25 and BAg-30 solder were statistically analyzed, and the Weibull fitting results are shown in Figure 9(c) and (d). In the shear and tensile tests, the scale parameters of BAg-25 are larger than those of BAg-30. BAg-25 has higher shape parameters in the tensile test than BAg-30, but lower shape parameters in the shear test. The results show that BAg-25 has higher breaking strength and smaller breaking dispersion in the tensile test. However, in the shear experiment, BAg-25 has a larger shear strength value and the fracture strength dispersion is higher than BAg-30.

The results show that the mechanical properties of BAg-25 brazed joint are obviously better than those of BAg-30 brazing joint. Because the size of the Cu-based solid solution in BAg-25 brazing joint is smaller than that in BAg-30 brazing joint, which is equivalent to grain refinement, there is no (Cu + Ag) eutectic phase formation in BAg-25 brazing joint [39].

4 Conclusion

The experimental results and analysis show that the mechanical properties of the new type BAg-25 flux-cored solder with lower silver content are better than those of BAg-30 flux-cored solder, which will further reduce the industrial cost.

The wettability of BAg-30 filler metal on the substrate increases with the increase in temperature and decreases after exceeding 850°C, which is better than BAg-25 in general. The maximum wetting areas of two kinds of metals appear at 850°C, that of BAg-30 is 374 mm^2 and that of BAg-25 is 275 mm^2. Both kinds of filler metals can achieve a good metallurgical bonding with substrate Q235, without microcracks and slag inclusion. However, both BAg-25 and BAg-30 are composed of copper-based and silver-based solid solutions, but the latter has a larger size microstructure interwoven with a small amount of needle-like eutectic silver-copper eutectic. Compared with the base metal, the microhardness of BAg-25 brazed joint is significantly increased, reaching 132.8 HV, and that of BAg-30 brazed joint is 125.8 HV. The tensile strength and the shear strength of BAg-25 brazed joint are generally higher than those of BAg-30 brazed joint, but the fracture dispersion of BAg-30 brazed joint in the shear test is better than that of BAg-25 brazed joint.

Acknowledgments: The authors gratefully acknowledge the funding from the Key Projects of Strategic International Scientific and Technological Innovation Cooperation (grant no. 2016YFE0201300); project (SKLABFMT201902) supported by the State Key Laboratory of Advanced Brazing Filler Metals and Technology, Zhengzhou Research Institute of Mechanical Engineering, Zhengzhou, China; project (20A43 0013) supported by the Education Department of Henan Province, China.

Conflict of interest: The authors declare no conflict of interest regarding the publication of this paper.

References

[1] Jia M, Weimin L, Peng H, Li B, Peng X, Mingfang W. Effect of gallium addition on microstructure and properties of Ag–Cu-Zn-Sn alloys. China Weld. 2015;24(3):6–10.
[2] Zhang L, Yu H, Ma J, Zhong SJ. Microproperties and interface behavior of the BAg25TS brazed joint. Vacuum. 2019;169:108928.
[3] Wierczyrczy A, Fydrych D, Rogalski G. Diffusible hydrogen management in underwater wet self-shielded flux cored arc welding. Int J Hydrog Energy. 2017;42(38):24532–40.
[4] Sun R, Zhu Y, Guo W, Peng P, Li L, Zhang Y, et al. Microstructural evolution and thermal stress relaxation of Al_2O_3/1Cr18Ni9Ti brazed joints with nickel foam. Vacuum. 2018;148:18–26.
[5] Huang S, Long WM, Lu QB, Jiu YT, Zhong SJ. Research on the corrosion resistance of Cu-Al joints brazed with flux-cored Zn-2Al filler metal. Mater Res Express. 2019;6:056560.
[6] Wang Y, Duan ZZ, Chen G, Jiang QY, Dong W, Lei K. Effects of brazing temperature on microstructure and properties of interface between cBN and Co-based active filler metals. Vacuum. 2017;145:30–8.
[7] López-Cuevas J, Rendón-Angeles JC, Rodríguez-Galicia JL. Interfacial reaction mechanism between molten Ag-Cu-based active brazing alloys and untreated or pre-oxidized PLS-SiC. Breast Cancer Online. 2019;4(57–58):3153–61.

[8] Cao J, Zhang LX, Wang HQ. Effect of silver content on microstructure and properties of brass/steel induction brazing joint using Ag-Cu-Zn-Sn filler metal. J Mater Sci Technol. 2011;27(4):377–81.
[9] Pawłowski R, Pawłowski B, Wita H, Pluta A, Sobik P, Sala A, et al. Ag nanoparticles in thermal silver-plating of aluminium busbar joints. Nanotechnol Rev. 2018;7(5):365–72.
[10] Yijie B, Yi Z, Yanlin J, Baohong T, Alex AV, Xiaohui Z, et al. Effects of Cr addition on the constitutive equation and precipitated phases of copper alloy during hot deformation. Mater & Des. 2020;191:108613. doi: 10.1016/j.matdes.2020.108613 (WOS:000536937200034).
[11] Gancarz T, Pstrus J. Formation and growth of intermetallic phases at the interface in the Cu/Sn-Zn-Ag-Cu/Cu joints. J Alloy Compd. 2015;647:844–56.
[12] Schnee D, Wiehl G, Starck S, Kevin C. Development of Ag-Cu-Zn-Sn brazing filler metals with a 10 weight-% reduction of silver and same liquidus temperature. China Weld. 2014;4:25–31.
[13] Mosstafa K, Massoud G, Ali M. Cobalt ferrite nanoparticles (CoFe2O4 MNPs) as catalyst and support: Magnetically recoverable nanocatalysts in organic synthesis. Nanotechnol Rev, 2018;7(1):43–68.
[14] Beura VK, Xavier V, Venkateswaran T, Kulkarni K. Interdiffusion and microstructure evolution during brazing of austenitic martensitic stainless steel and aluminum-bronze with Ag-Cu-Zn based brazing filler material. J Alloy Compd. 2018;740:852–62.
[15] Winiowski A, Rózanski M. Impact of tin and Nickel on the brazing properties of silver filler metals and on the strength of brazed joints made of stainless steels. Arch Metall Mater. 2013;58(4):1007–11.
[16] Xiong H, Tan Z, Zhang R, Zong Z, Luo Z. Flexural behavior and mechanical model of aluminum alloy mortise-and-tenon T-joints for electric vehicle. Nanotechnol Rev. 2019;8(1): 370–82.
[17] Khorunov VF, Stefaniv BV, Maksymova SV. Effect of nickel and manganese on structure of Ag-Cu-Zn-Sn system alloys and strength of brazed joints. Paton Weld J. 2014;4:22.
[18] Chaoli M, Xue S, Bo W. Study on novel Ag-Cu-Zn-Sn brazing filler metal bearing Ga. J Alloy Compd. 2016;688:854–62.
[19] Irena B, Janja S, Uroš M. NiCu magnetic nanoparticles: review of synthesis methods, surface functionalization approaches, and biomedical applications. Nanotechnol Rev. 2018;7(2):187–207.
[20] Qi JL, Wang ZY, Lin JH, Zhang TQ, Zhang AT, Cao J. Graphene-enhanced Cu composite interlayer for contact reaction brazing aluminum alloy 606. Vacuum. 2016;136:142–5.
[21] Kole KoR, Chachula M. Characteristics and properties of Bi-11Ag solder. Soldering Surf Mt Technol. 2013;25(2): 68–75.
[22] Chaoli M, Xue S, Bo W. Study on novel Ag-Cu-Zn-Sn brazing filler metal bearing Ga. J Alloy Compd. 2016;688:854–62.
[23] Feng J, Liang S, Guo X, Zhang Y, Song K. Electrical conductivity anisotropy of copper matrix composites reinforced with SiC whiskers. Asia Pac J Risk Insurance. 2019;8(1):285–92.
[24] Lubomir L, Martin V, Barbora L. Materials characterization of advanced fillers for composites engineering applications. Nanotechnol Rev. 2019;8(1):503–12.
[25] Bobylev SV, Sheinerman AG. Effect of crack bridging on the toughening of ceramic/graphene composites. Rev Adv Mater Sci. 2019;57.
[26] Chen Y, Yun D, Sui F. Influence of sulphur on the microstructure and properties of Ag–Cu–Zn brazing filler metal. Mater Sci Technol (Lond). 2013;29(10):1267–71.
[27] Dimitrijevi SP, Manasijevi D, Kamberovi, Dimitrijevi SB, Mitri M, Gorgievski M. Experimental investigation of microstructure and phase Transitions in Ag-Cu-Zn brazing alloys. J Mater Eng Perform. 2018;27:1570–9.
[28] Bobruk EV, Sauvage X, Zakirov AM, Enikeev NA. Tuning the structure and the mechanical properties of ultrafine grain Al–Zn alloys by short time annealing. Rev Adv Mater Sci. 2019;55.
[29] Xue P, Zou Y, He P, Pei Y, Sun H, Ma C, Luo J. Development of low silver AgCuZnSn filler metal for Cu/steel dissimilar metal joining. Metals. 2019;9(2):198.
[30] Yongfeng G, Yi Z, Kexing S, Yanlin J, Xu L, Heinz-Rolf S. Effect of Ce addition on microstructure evolution and precipitation in Cu-Co-Si-Ti alloy during hot deformation. J Alloy Compd. 2020;842(11):155666. doi: 10.1016/j.jallcom.2020.155666 (WOS:000512369200047).
[31] Yang J, Lee H, Choi AR, Park KH, Ryu JH, Oh EJ. Comparison of allergen-specific IgE levels between immulite 2000 and ImmunoCAP systems against six inhalant allergens and ten food allergens. Scand J Clin Laboratory Investigation. 2018;78(7–8):606–12.
[32] Xia C, Sun W, Zhou Y, Xu X. Thermal fatigue damage and residual mechanical properties of W-Cu/Ag-Cu/1Cr18Ni9 brazed joint. J Alloy Compd. 2018;741:155–60.
[33] Feng J, Liang S, Guo X, Zhang Y, Song K. Electrical conductivity anisotropy of copper matrix composites reinforced with SiC whiskers. Asia Pac J Risk Insurance. 2019;8(1):285–92.
[34] Konakov VG, Yu. Kurapova O, Solovyeva EN. Synthesis, structure and mechanical properties of bulk “Copper-Graphene” composites. Rev Adv Mater Sci. 2018;57.
[35] Norouzi E, Shamanian M, Atapour M. Diffusion brazing of Ti–6Al–4V and AISI 304: an EBSD study and mechanical properties. J Mater Sci. 2017;52(20):12467–75.
[36] Xiaohui Z, Yi Z, Kexing S, Yanlin J, Xiaohong C. Review of nanophase effects in high strength and conductivity copper alloys. Asia Pac J Risk Insurance. 2019;8(1):383–95.
[37] Guangyu Z, Dao W, Yao X, Jiamu D, Wei Z. Fabrication of Ag Np-coated wetlace nonwoven fabric based on amino-terminated hyperbranched polymer. Asia-Pacific J Risk Insurance. 2019;8(1):100–6.
[38] Xiong H, Tan Z, Zhang R, Zong Z, Luo Z. Flexural behavior and mechanical model of aluminum alloy mortise-and-tenon T-joints for electric vehicle. Nanotechnol Rev. 2019;8(1):370–82.
[39] Kozlova O, Braccini M, Voytovych R. Brazing copper to alumina using reactive CuAgTi alloys. Acta Mater. 2010;58(4):1252–60.